Spring 2013

Paste development and co-sintering test of zirconium carbide and tungsten in Freeze-form Extrusion Fabrication

Ang Li

Department:

PASTE DEVELOPMENT AND CO-SINTERING TEST OF ZIRCONIUM CARBIDE AND TUNGSTEN IN FREEZE-FORM EXTRUSION FABRICATION

by

ANG LI

A THESIS

Presented to the Faculty of the Graduate School of the
MISSOURI UNIVERSITY OF SCIENCE AND TECHNOLOGY
In Partial Fulfillment of the Requirements for the Degree

MASTER OF SCIENCE IN MANUFACTURING ENGINEERING

2013

Approved by

Ming C. Leu, Advisor
Greg E. Hilmas
Robert G. Landers

ABSTRACT

Ultra-high temperature ceramics are being investigated for future use in aerospace applications due to their superior thermo-mechanical properties, as well as oxidation resistance, at temperatures above 2000 ℃. However, their brittle properties make them susceptible to thermal shock failure. Components fabricated as functionally graded materials (FGMs) can combine the superior properties of ceramics with the toughness of an underlying refractory metal by fabricating graded composites. This paper discusses the grading of two materials through the use of a Freeze-form Extrusion Fabrication (FEF) system to build FGMs parts consisting of zirconium carbide (ZrC) and tungsten (W). Aqueous-based colloidal suspensions of ZrC and W were developed and utilized in the FEF process to fabricate test bars graded from 100%ZrC to 50%W-50%ZrC (volume percent). Following FEF processing the test bars were co-sintered at 2300 ℃ and characterized to determine their resulting density and micro-structure. Four-point bending tests were performed to assess the strength of test bars made using the FEF process, compared to test bars prepared using conventional powder processing and isostatic pressing techniques, for five distinct ZrC-W compositions. Scanning electron microscopy (SEM) was used to verify the inner structure of composite parts built using the FEF process.

ACKNOWLEDGEMENT

First I would like to express my gratitude to my advisor, Dr. Ming Leu, who brought me into this project and gave me generous support and guidance. I would also like to thank Dr. Greg Hilmas and Dr. Jeremy Watts for sharing their knowledge with me, kindly offering me support for research, and tolerating me for frequent visit for questions. I would also like to thank Dr. Robert Landers for his kind advices and support during my graduate study. Never in my life have I seen such devoted and enthusiastic attitude towards knowledge like theirs. They set a significant example with their diligence and outstanding academic performance, teaching me how to be a successful engineer in my future career.

I would like to thank my colleagues from the ceramic engineering department, Jaci Huebner, Eric Neuman and Britteny Voss for offering help and sharing their knowledge with me during my study.

I would like to thank my fellow students Mingyang Li, Brad Deuser, Aaron Thornton, Diego Garcia, Nannan Guo, Max Mulholland and Krishna Kolan for their help, support, and friendship throughout my graduate work.

My parents, Guangmei Li and Zhengqun Zhou, have been a constant source of support with their words of encouragement and praise.

Last, but not least, I would like to thank my wife Pu for her love and patience in the past several years as she has been supportive throughout my undergraduate and graduate studies.

TABLE OF CONTENTS

Page

LIST OF ILLUSTRATIONS

Page

LIST OF TABLES

Page

1. INTRODUCTION

Fabrication of a functionally graded material (FGM) part refers to the process of manufacturing a part with multiple materials in a graded fashion in order to take advantage of complementary material properties while minimizing residual stresses that may result from the sintering process [1]. Ceramics are often used in high-temperature applications for their superior heat resistance; however, poor fracture toughness limits their use in high-stress scenarios and they are often difficult to manufacture for complex geometries using traditional processes. Several additive manufacturing technologies have been developed in recent years that can fabricate complex geometry ceramic components, but few have the ability to build FGM parts.

Additive manufacturing (AM) technology has evolved since its inception in the mid 1980's, from polymer-based processes to metal-based and ceramic-based processes. Stereolithography [2], Fused Deposition Modeling [3], 3D printing [4], and Selective Laser Sintering [5,6] are among the popular AM technologies practiced in industry today. The current metal and ceramic AM technologies are mostly limited to single material (monolithic) part fabrication. Robocasting [7], Extrusion Freeform Fabrication [8], Shape Deposition Manufacturing [9], and Laser Metal Deposition [10] are more apt in their potential to building multiple-material parts since they are deposition-based processes.

This study considers a novel additive manufacturing technology called Freeze-form Extrusion Fabrication (FEF), which is capable of producing three-dimensional parts by depositing aqueous-based ceramic and metal pastes in a layer-by-layer manner within a sub-zero temperature environment to minimize the amount of binder necessary, thus making post-processing easier and more environmentally friendly [11-15].

Some key components in aerospace applications demand extremely high performance, such as the leading edges of hypersonic vehicles, missile nose cones, and nozzle throat inserts for spacecraft propulsion systems. These components must be able to withstand extremely high temperatures (> 2000 ℃) and be integrated with underlying substructures, which are typically made of metals such as aluminum or titanium. To achieve these demanding characteristics, one approach is to build these components while grading from a ceramic to a metal. The grading should be done in a gradual fashion so as to minimize the thermal stresses generated due to different thermal expansion coefficients between the different materials, both during part fabrication and when the part is in service. Deposition-based additive manufacturing processes are advantageous for fabricating such components with functionally graded materials (FGMs).

This paper considers the sintering of ZrC-W composite parts fabricated by the FEF process. As a refractory metal with a melting point of 3422 ℃ and yield strength of approximately 800 MPa at room temperature [17], W shows great potential in aerospace applications such as re-entry components, uncooled liquid rocket chambers, rocket nozzles, electrical propulsion components, etc. However, there will be a dramatic decrease in the mechanical strength of W with a rise in temperature [17]. For example, the mechanical strength of W decreases by ~60% when heated from room temperature to 1000 ℃ [17]. To enhance the mechanical strength of W in elevated temperature, ZrC can be introduced as a reinforcement material because of its high melting temperature (3532 ℃) and similar thermal expansion coefficient as W [18]. Several methods have been used for the fabrication of ZrC-W composites, the most typical one being hot pressing [18]. A high relative density can be achieved by the hot pressing method (＞

98%); however, the dimensional limitation narrows the scope of applications for this method. An in-situ reaction sintering process was able to achieve a relative density of approximately 94.5% for the manufacture of ZrC-W composites without applying external pressure during sintering [19]. In this paper, we compare the relative densities, flexural strengths, and microstructures of test bars of different ZrC and W compositions fabricated by the FEF process and by a traditional powder processing route that includes isostatic pressing. The test bars were sintered at temperatures ranging from 2100 to 2300 ℃ in attempts to achieve the highest possible relative densities.

The FEF process uses aqueous pastes as the extrude material, which demands homogeneous dispersion of particles in the paste. In previous studies, aqueous pastes of other materials, such as alumina (Al_2O_3), zirconia (ZrO_2), etc., have been successfully developed and applied in additive manufacturing [13-16, 20-21], but there is no previous experience on the development of tungsten paste. The challenge of this study is to get tungsten well dispersed in water, which is difficult because of its high density. Based on the previous experience in paste development, a slight change in the composition and process parameters could greatly affect the extrusion behavior of a paste. The goal of this study is to develop a repeatable and reliable recipe to produce high-quality ZrC and W pastes for the FEF process.

Another challenge in this study is the co-sintering of zirconium carbide and tungsten. The strong covalent bonding of zirconium carbide prevents this material from achieving high density through conventional sintering techniques [22]. Hot pressing has been the most typical method in the heat treatment of zirconium carbide [22-24]. However, the limitation of part dimensions narrows the application of hot pressing. Due

to different material properties, zirconium carbide and tungsten exhibit different densification behavior during heat treatment. In this thesis, several heating conditions were tested to find the best parameters that enable both materials to reach high density and good mechanical strength.

2. FREEZE FORM EXTRUSION FABRICATION PROCESS OVERVIEW

An FEF machine equipped with three servo controlled extruders and a three-axis gantry motion system in a temperature-controlled enclosure has been developed, as shown in Figure 2.1. The FEF machine is equipped with a triple-extruder mechanism to build three-dimensional FGM parts with complex geometries. The different materials are combined by feeding them into an inline static mixing unit and output the mixed pastes through a single orifice. This static mixer forces the pastes to mix together before exiting the orifice, and provides a natural transition between paste composition changes. The different pastes are extruded simultaneously by controlling the velocity of each plunger. As an example, assuming that the three cylinders contain three different pastes and have the same cross-sectional area, a desired paste mixture consisting of 20% paste A, 30% paste B, and 50% paste C can be achieved by controlling the three plunger velocities with the ratios of v1:v2:v3 = 2:3:5, where v1, v2, and v3 are the plunger velocities for pastes A, B, and C, respectively. The mixed colloidal paste is deposited onto a solid substrate layer by layer within a sub-zero temperature environment (-10 ℃ in our present study). Following the FEF fabrication, the fabricated part is transferred to a freeze-dryer to sublime excess water from the green part and then undergoes binder burnout and sintering.

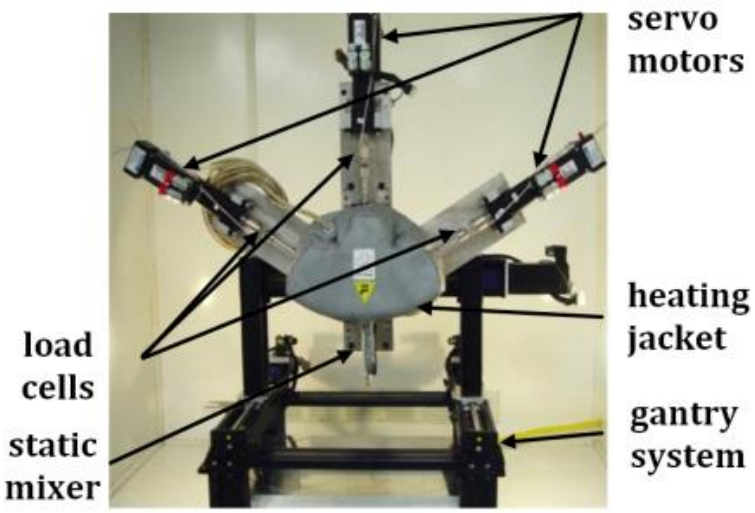

Figure 2.1. The triple-extruder Freeze-form Extrusion Fabrication (FEF) machine.

3. MATERIALS PROCESSING

3.1. POWDER CHARACTERIZATION

The identification of properties of powders is important because of their significant effect on the process of paste. The characterization tests in this study include surface area analysis (BET) and particle size analysis. Each batch of powder (including different lot numbers) was tested for comparison within each material. Table 3.1 lists all the raw materials used for testing, which includes the company, type of powder, and lot number. The zirconium carbide powder was attrition-milled based on the sintering performance which will be discussed in next chapter. The zirconium carbide powder was first poured into a beaker with tungsten carbide media and acetone, which were mixed for around 2 hours, followed by a drying process with a rotavapors (Model# RE114, Buchi, Germany). The dry powder went through an 80 mesh sieve and was stored for future use.

Table 3.1. Raw Materials Included in Characterization tests

Material Name	Company	Powder Type	Lot #
Tungsten #1	Aldrich	510106-500G	MKBH4155V
Tungsten #2	Aldrich	510106-500G	12224EE
Zirconium Carbide	H.C. Starck	Grade B AB134580	25052/11
Zirconium Carbide (Attrition milled)	H.C. Starck	Grade B AB134580	25052/11

3.1.1. BET Surface Area. The Brunauer, Emmett, and Teller (BET) surface area analysis is a technique used to determine the surface area of powders. The values are expressed in m^2/g. It is important to measure the particle surface area since a higher surface area may result in higher densification during sintering. The machine used is a NOVA Surface Area Analyzer (NOVA 1000, Quantachrome, Boynton Beach, FL). The BET surface analysis uses the gas sorption method to determine the surface area of the particle. The particle of the powder was firstly cleaned by using a heating vacuum or flowing gas. Once the particles of the powder were cleaned, a gas adsorbs over the entire exposed surface of the powder particles. The machine analyzed the amount of gas molecules covering on the powder particles to calculate the surface area. After the measurement, the surface area and the correlation coefficient were recorded. The NOVA surface area analyzer is able to test two specimens at the same time.

The results of surface area measurement are listed in Table 3.2, it is shown that even from the same company, different lots of the same material (tungsten) still may have varying properties. The table also shows that the surface area of zirconium carbide powder was greatly increased after the attrition mill.

Table 3.2. Surface area measurement results for the materials under consideration

Material	Surface Area (m^2/g)	Correlation Coefficient
Tungsten #1	1.457	0.999856
Tungsten #2	1.922	0.999858
ZrC	1.061	0.999918
Attrition milled ZrC	6.132	0.999927

3.1.2. Particle Size Analysis. The particle size analysis in this study was performed using the Microtrac Particle Size Analyzer (S3500, Microtrac, Montgomeryville, PA). The intention of this measurement is to define the particle size of a given powder for purposes of investigating in effects of particle size on paste development and sintering process.

The particle sizes of the measured powders are listed in Table 3.3, and the particle size distributions are shown in Figures 3.1 and 3.2. When comparing the different tungsten materials in 3-1, different dispersants and concentrations would be needed for the different types of tungsten because of their varying particle size distributions and surface areas (in Table 3.3). Tungsten #2 has a smaller size range, shown by the peak, while having a larger surface area between the two tungsten powders. The larger the surface area, the more difficult to disperse the powder to make paste, therefore tungsten #1 is a better choice in paste development than tungsten #2.

The average particle size of ZrC was decreased from 0.469 μm to 0.348 μm after attrition milling, which increased surface area from 1.061 m^2/g to 6.132 m^2/g. Taking consideration of the paste development, as-received ZrC powder tends to be a better choice for its lower surface area which will make the dispersion easier, but during sintering (to be discussed later), attrition milled ZrC powder showed a significant advantage in the densification, since the dispersion of attrition milled ZrC did not present any difficulty, attrition milled ZrC powder was chosen as the material used in both paste development and sintering test in this study (to be discussed in the next section). The standard for choosing the suitable ZrC powder is different from W powder, bacause W is

a metal material and shows great advantage in the densification during sintering against ZrC, which is a ceramic material.

Table 3.3. Particle size measurement results for the materials under consideration

Material	Particle size (µm)
Tungsten #1	0.832
Tungsten #2	0.576
ZrC	0.469
Attrition milled ZrC	0.348

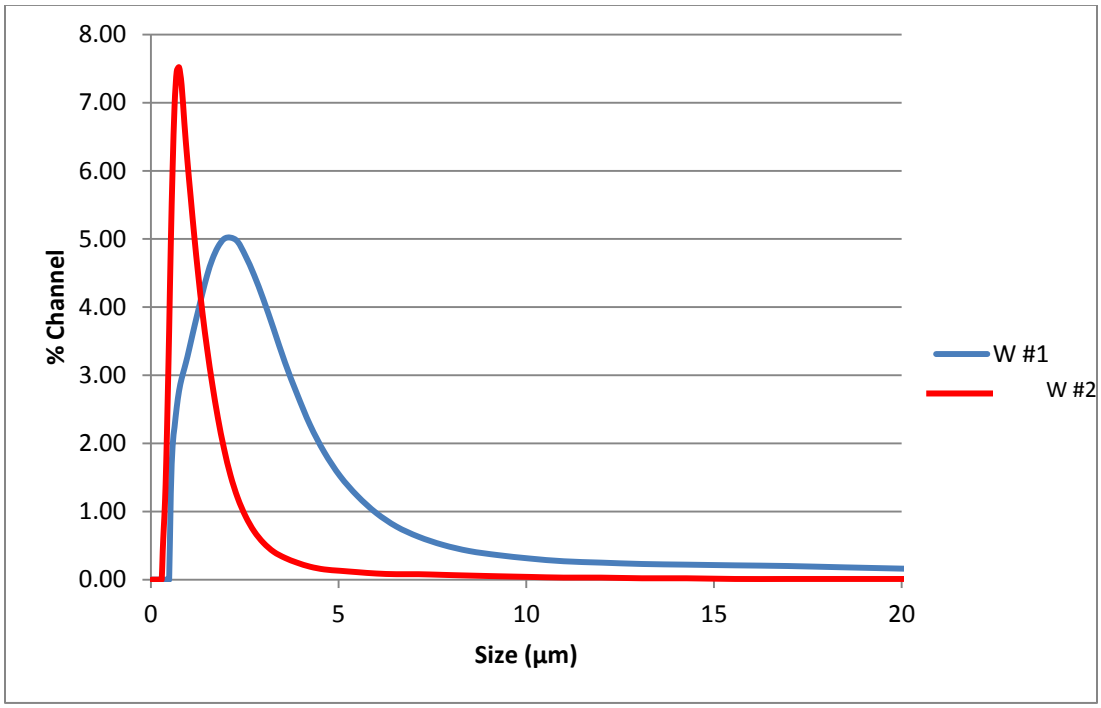

Figure 3.1. Particle size analysis results for the tungsten powders

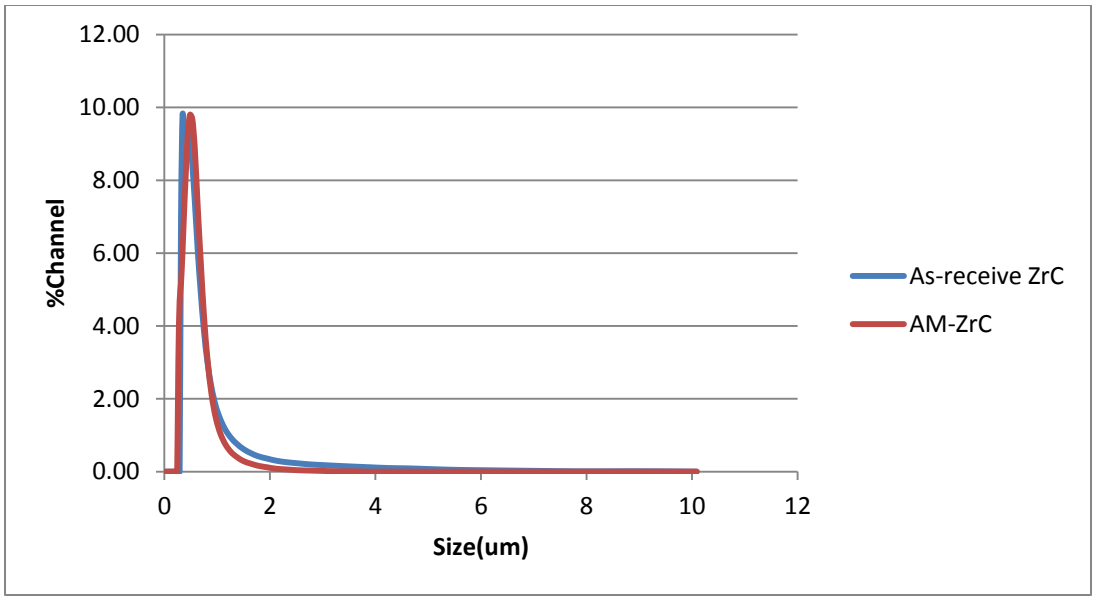

Figure 3.2. Particle size analysis for the as-received and attrition milled zirconium carbide powder

3.1.3. Dispersion Test. The most challenging issue in the paste development is to find a suitable dispersant that works for both zirconium carbide and tungsten powders. Based on the previous work done by Dr. Jeremy Watts and Brittney Voss on the selection of dispersant, sodium dodecyl sulfate (Sigma Aldrich, St. Louis, MO), Castament FS 10, Castament FS 20, Melflux 2651F and Melment F10 (BASF, Germany) were tested as the candidate dispersants in the development of tungsten pastes. The reason of choosing those dispersants was because that they are all polycarboxylate. Their backbone, which is negatively charged, permits the adsorption on the positively charged particle surfaces. As a consequence of the adsorption, the zeta potential of the suspended particles changes, due to the adsorpsion of the COO^- groups on the colloid surface. This displacement of the polymer on the particle surfaces ensures to the side chains the possibility to generate repulsion forces, which disperse the particles of the suspension and avoid friction. Since most of dispersants could work well with ZrC, only W powder was tested in this experiment.

In the dispersant test, a beaker was put on the top of a magnetic plate. The beaker had a stirring bar inside, 10 ml of water was poured into the beaker and the stirring speed was set to 80 rpm. The objective of this experiment was to find out which dispersant could reach the highest solid loading of W in the slurry at the same dispersant concentration (dispersant: surface area of W powder = $1 mg/m^2$). 157.5 g W powder (45 vol% solids loading if the entire amount is dispersed in water) was prepared for each dispersant. Accordingly, ~0.22 g of dispersant was added into the water before adding W powder. Then W powder was slowly added into the beaker with a spatula. The amount of

W powder added into the water when the stirring bar stopped was recorded and the solid loading was calculated. The results are giving in Table 3.4.

Table 3.4. Dispersion test of tungsten powder

Dispersant	**Amount of tungsten powder added (g)**	**Corresponding solids loading (vol%)**
Sodium Dodecyl Sulfate (SDS)	138.4	41.8
Castament FS 10	25.3	N/A
Castament FS 20	85.3	30.7
Melflux 2651F	70.1	26.7
Melment F10	31.2	13.9

There is no result for the Castament FS 10 added slurry because the W particles formed agglomerations soon after they were added into the beaker. Among all these dispersant candidates, sodium dodecyl sulfate (SDS) showed the best result, the slurry remained in good fluidity even after the stirring bar stopped and there was no visual agglomeration inside the beaker. Thus SDS was shown to be the most efficient dispersant for W. The same test was performed on ZrC powder usint SDS as the dispersant, in which the solid loading reached ~55%. Thus SDS was chosen for the development of W and ZrC pastes.

3.1.4. Discussion. Based on the characterization of powders, the recipes for making zirconium carbide and tungsten paste were developed based on the previous alumina recipe developed by Brittney Voss and Ana Alvarez in their REU project during the 2011 summer (see appendices). The zirconium carbide and tungsten paste were successfully developed at the solids loading of ~50%, which showed good extrusion behavior in the triple extruder machine.

During the paste development, we try to conclude a standard that could be referred judge if a paste is a "good" one. However, since the properties of different powders vary so much, we could only define a "good" paste by the extrusion behavior. According to the data during the FEF process, the typical extrusion force of "good" paste stays at around 600N, and there will be no dramatic change in the force caused by clogging and air bubbles.

The reason of increasing solids loading of pastes is to enhance the density of sintered parts and eliminate the porosity as much as possible. Since the porosity inside the parts is mainly caused by the evaporation of water, the decrease in water content should be able to bring down the porosity. And a better mechanical strength of sintered parts is expected by increasing the solids loading of pastes.

3.2. CHARACTERIZATION OF SINTERING BEHAVIOR

In order to achieve acceptable mechanical properties, ZrC-W composites produced by the FEF process will require a high temperature sintering cycle to achieve the highest possible relative density. The co-sinterability of ZrC and W was investigated by fabricating several batches of test pellets with the composition of 50vol%ZrC+50vol% W and sintering at different temperatures and heating rates (as shown in Table 3.5).

During the experiments, the powders of ZrC (＜2μm, Grade B, H.C. Starck, Karlsruhe, Germany) and W (0.6~1μm, Sigma Aldrich, St. Louis, MO) were first mixed and ball-milled using acetone and zirconia media for 2 hours. After ball milling, the slurry was dried by rotary evaporation (Buchi, Flawil, Germany) at a temperature of 70 ℃, low vacuum (~27 kPa), and a rotation speed of 60 rpm. The dry powder was ground, filtered through a 180μm sieve, and pressed into pellets using a hydraulic press with a half-inch diameter die at 2000 psi. The pellets were then isostatically pressed at 30,000 psi before being placed in a graphite crucible for sintering. Sintering was performed in a graphite furnace (Thermal Technology, Santa Rosa, CA) under a helium atmosphere. The densities of the sintered pellets were determined using the Archimedes method, and each pellet was polished for scanning electron microscopy (SEM, S4700 and S570, Hitachi, Tokyo, Japan). Figure 3.3 shows the pressed and sintered pellets.

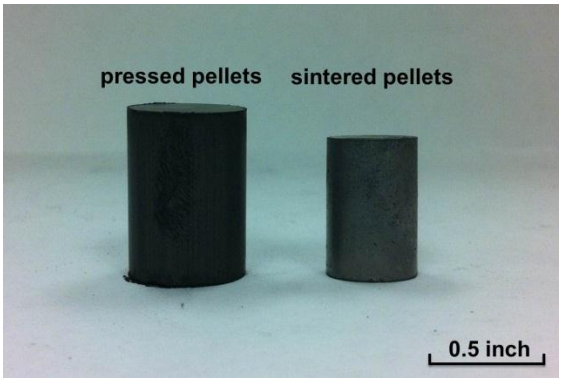

Figure 3.3. Pressed and sintered pellet

The sintering of the pellets (co-sintering of ZrC and W) was performed under four different heating conditions, which are listed along with the resulting relative density data in Table 3.5. Maintaining a heating rate of 10 ℃/min and increasing the sintering

temperature from 2100 ℃ to 2300 ℃ was found to increase the relative density from ~71% to ~83%. However, a relative density above 83% could not be achieved despite additional changes to the sintering cycle. SEM analysis of a sample with the highest relatively density (~83%) showed many visible pores in the ZrC phase as seen in Figure 3.4 where ZrC is the darker phase and W is the lighter phase. This indicates that the rate of grain growth of ZrC was too fast under the current heating condition, causing entrapped porosity and thus insufficient densification of ZrC. To enhance the driving force for densification of ZrC at lower temperatures, attrition milling was introduced to reduce the particle size and increase the surface area of ZrC. The detail has been introduced in last chapter.

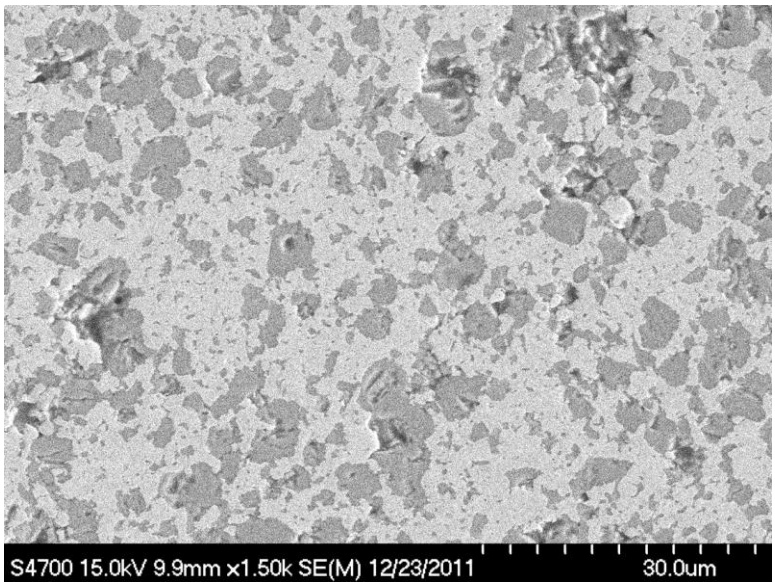

Figure 3.4. SEM images of 50%ZrC+50%W pellets with relative density of 82.59%

Table 3.5. Heating conditions for co-sintering test

Temperature	Holding time	Atmosphere	Heating rate	Relative density
2100 ℃	1 hour	Helium	10 ℃/min	74.51%
2300 ℃	1 hour	Helium	10 ℃/min	71.52%
2300 ℃	3 hours	Helium	10 ℃/min	80.71%
2300 ℃	3 hours	Helium	10 ℃/min from room temperature to 2100 ℃, and then 2 ℃/min to 2300 ℃	82.59%

To verify the effect of these changes on the sinterability of ZrC, another batch of pellets was made with the composition of 50vol%ZrC+50vol%W and 90vol%ZrC+10vol%W using the attrition milled ZrC powder. Also, one batch of 90vol%ZrC (as-received)+10vol%W pellets were also produced for comparison. The sintering test was conducted at a heating rate of 10 ℃/min from room temperature to 2100 ℃, and then 2 ℃/min to 2300 ℃ in order to allow for more time at the lower sintering temperatures and limit ZrC grain growth.

The density of the pellets made with attrition-milled ZrC powder resulted in a significant increase in the density compared with the pellets made with the as-received ZrC powder (Table 3.6). The 50vol%ZrC+50vol%W composition achieve a ~99% relative density, while the 90vol%ZrC+10vol%W composition achieved a relative density of 99.4%. Figure 3.5 shows SEM images for 50vol%ZrC+50vol%W pellets made with

as-received and attrition-milled ZrC powders. Based on SEM analysis, it is clear that attrition milling not only contributed to a higher density after sintering, but also decrease the resulting ZrC and W grain sizes. The number and size of pores inside the sintered parts were also reduced. Attrition milling increased both the surface area of particles and the concentration of defects, resulting in higher diffusion coefficient and shorter diffusion distance for the ZrC powder. Thus, the sintered pellets made with attrition-milled ZrC powder resulted in a higher density and finer microstructure.

Table 3.6. Comparison between sintered pellets made with as-received and attrition-milled ZrC powder

Composition	Relative density (with as-received ZrC)	Relative density (with attrition-milled ZrC)
50vol%ZrC+50vol%W	82.59%	98.9%
90vol%ZrC+10vol%W	71.32%	99.4%

ZrC/W sintered pellets, made using the attrition-milled ZrC powder, were ground back to powder for X-ray diffraction (XRD) analysis (XDS 2000, Scintag Inc., Cupertino, CA) and the XRD results are included as Figure 3.6 The detected, highest intensity ZrC peaks (55.841^{o}, 66.612^{o}, 69.985^{o} and 82.921^{o}) in the XRD patterns were all shifted to higher two-theta angles compared to the reference peaks (55.633^{o}, 66.348^{o}, 69.712^{o} and 82.589^{o}). An increase in the two-theta angle indicates a decrease in lattice parameter in the ZrC unit cell, implying that there was formation of (Zr,W)C solid solution. This is not an unexpected result and has been previously observed in the technical literature for ZrC-W systems[19].

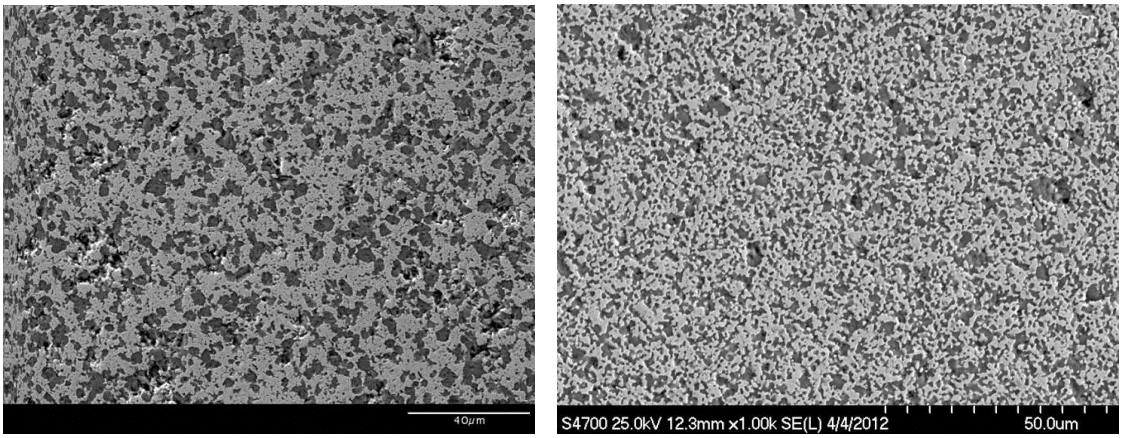

(a) **(b)**

Figure 3.5. Micro-structure of 50vol%ZrC+50vol%W pellets (a). made from as-received ZrC powder; (b) made from attrition-milled ZrC powder.

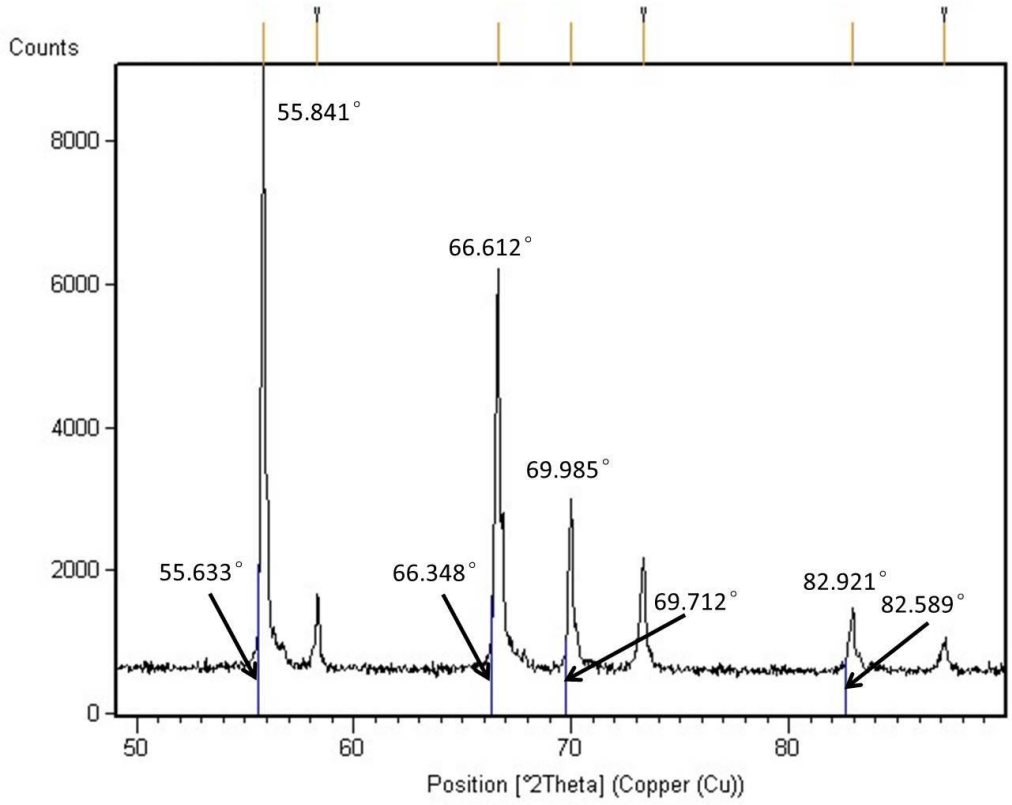

Figure 3.6. XRD analysis on ZrC/W pellets

3.3. FEF TEST BAR FABRICATION

Test bars of five different compositions were fabricated using the FEF process, among which three compositions, 12.5vol%W+87.5vol%ZrC, 75vol%W+25vol%ZrC and 37.5vol%W+62.5vol%ZrC were deposited by mixing of the two initial pastes (100vol%ZrC and 50vol%ZrC+50vol.%W) in various ratios.. Five additional test bars were made using an isostatic press after mixing W and attrition-milled ZrC powders into the desired compositions for comparison of mechanical properties. The process of fabricating test bars was the same as that for pellets. After sintering, these test bars were cut and ground into 3×4×45 mm3 pieces according to ASTM C 1161-02c for type B bars.

From the data in Table 3.7 it can be seen that for the isostatic pressed bars, the flexural strength increased for a higher concentration of W, increasing from ~224 for 100% ZrC to 404 MPa for the 50:50 ZrC:W composition. This result implies that the W played an important role in strengthening the composites. For the FEF fabricated bars this trend does not hold true. However, the relative density and flexural strength of FEF fabricated bars were, in general, much lower than those of the isostatic pressed bars. In order to have a better understanding of the differences, SEM images were taken to compare the microstructures of the test bars. From the SEM analysis (Figure 3.7), many large pores (10's to 100's of μm) were present in the bars produced by the FEF process. Further, the porosity became even more severe with increasing ZrC content. However, all of the isostatic pressed bars show highly densified microstructures, with relative densities all above 94% and the 50:50 ZrC:W composition achieving ~99.8%.

Table 3.7. Measured properties of FEF fabricated and iso-pressed test bars

	FEF Fabricated		Isostatic Pressed	
Composition (vol.%)	Relative Density	Flexural Strength (MPa)	Relative Sintered Density	Flexural Strength(MPa)
100%ZrC	62.05%	73	98.49%	224
12.5%W+87.5%ZrC	47.89%	25	94.41%	265
25%W+75%ZrC	56.19%	25	97.34%	398
37.5%W+62.5%ZrC	47.28%	28	95.40%	414
50%W+50%ZrC	70.08%	31	99.81%	404

There are two reasons for the severe porosity in the FEF fabricated bars. The first reason is that the static mixer did not do an adequate job of mixing the pastes, leading to significant variations in the materials compositions and differential sintering at different locations within the test bars. Figure 3.8 shows the cross sections of FEF fabricated test bars with 62.5%ZrC+37.5%W and 87.5%ZrC+12.5%W. Clearly visible in the images are marked differences in the intended compositions at different locations. The ZrC-rich areas (darker phase) are distinct from W-rich areas (lighter phase), indicating the insufficient paste mixing during extrusion. The second and more critical reason for the porosity is that during the FEF process large ice crystals were formed as the water was freezing. This has been shown in previous studies of aqueous based freeze casting of ceramics wherein large ice crystals are formed, resulting in large voids (100's of μm) after sintering [20]. Once formed during the freezing process, these large defects

remained inside the test bars, affecting the final mechanical properties. An example is given in Figure 3.9, which shows the formation of what appears to be the remnants of ice crystals (similar to Sofie and Dogan, ref [20]) in the 100% ZrC sample after freeze drying. As has been discussed by Sofie and Dogan, these voids may be controlled, or eliminated, in the future through the use of glycerol additions to the aqueous based slurries.

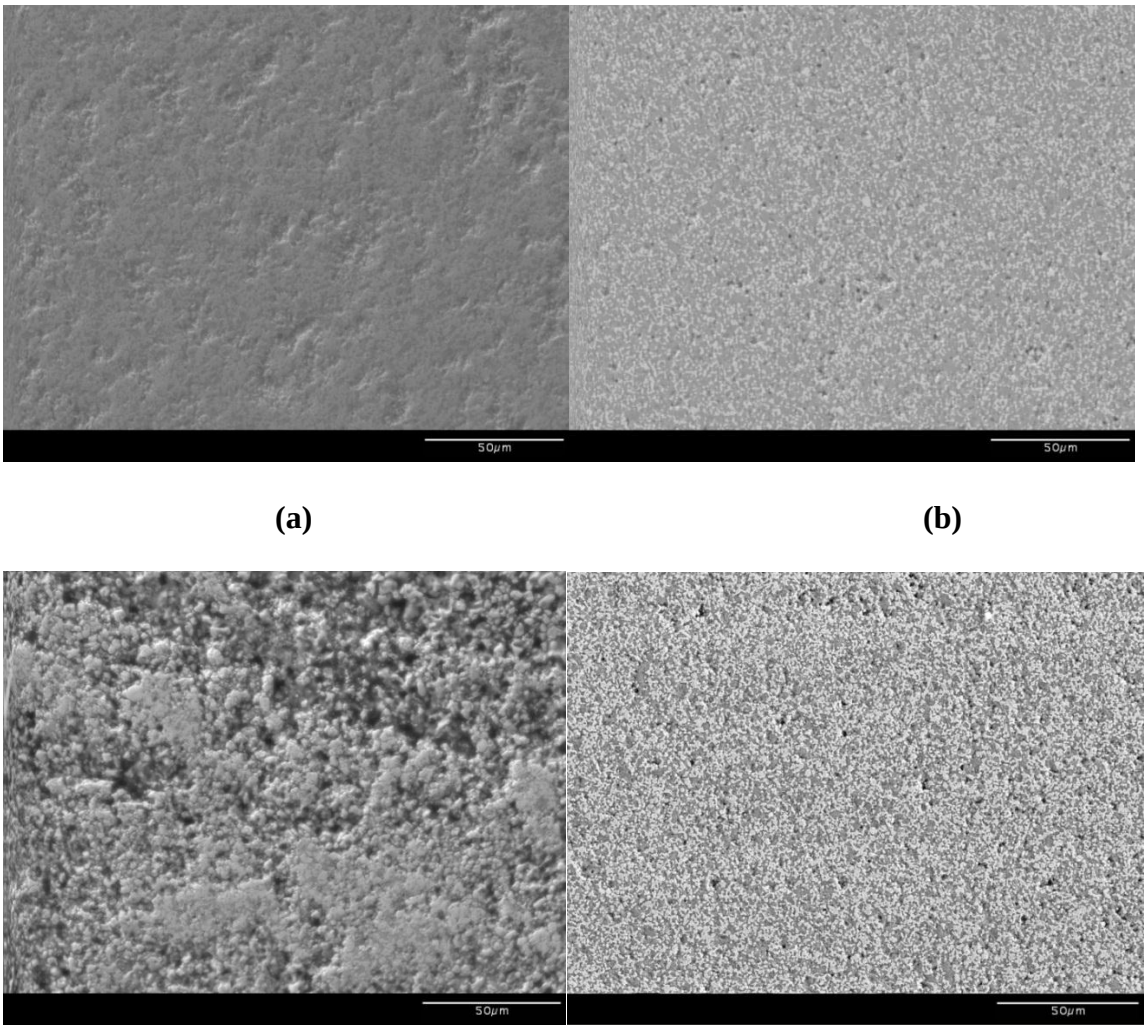

(a) **(b)**

(c) **(d)**

Figure 3.7. SEM images of the micro-structure of (a). 50%ZrC+50%W, FEF fabricated; (b). 50%ZrC+50%W, isostatic pressed; c). 62.5%ZrC+37.5%W, FEF fabricated; (d). 62.5%ZrC+37.5%W, isostatic pressed; (e). 75%ZrC+25%W, FEF fabricated; (f). 75%ZrC+25%W, isostatic pressed; (i). 100%ZrC, FEF fabricated; (j). 100%ZrC, isostatic pressed

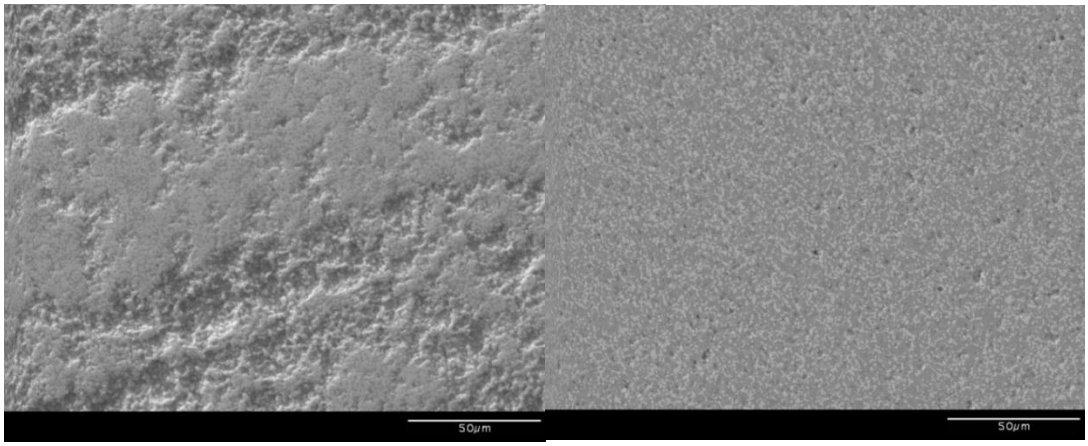

(e) **(f)**

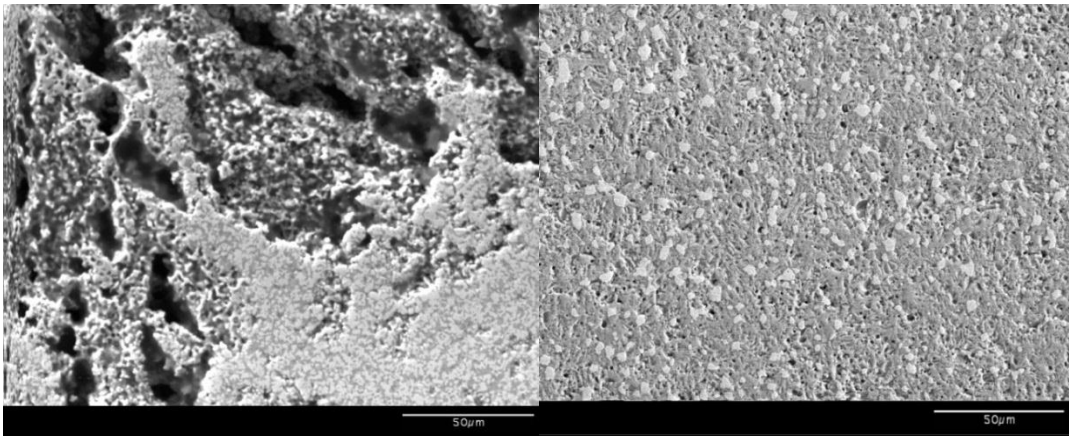

(g) **(h)**

Figure 3.7. SEM images of the micro-structure of (a). 50%ZrC+50%W, FEF fabricated; (b). 50%ZrC+50%W, isostatic pressed; c). 62.5%ZrC+37.5%W, FEF fabricated; (d). 62.5%ZrC+37.5%W, isostatic pressed; (e). 75%ZrC+25%W, FEF fabricated; (f). 75%ZrC+25%W, isostatic pressed; (i). 100%ZrC, FEF fabricated; (j). 100%ZrC, isostatic pressed (cont)

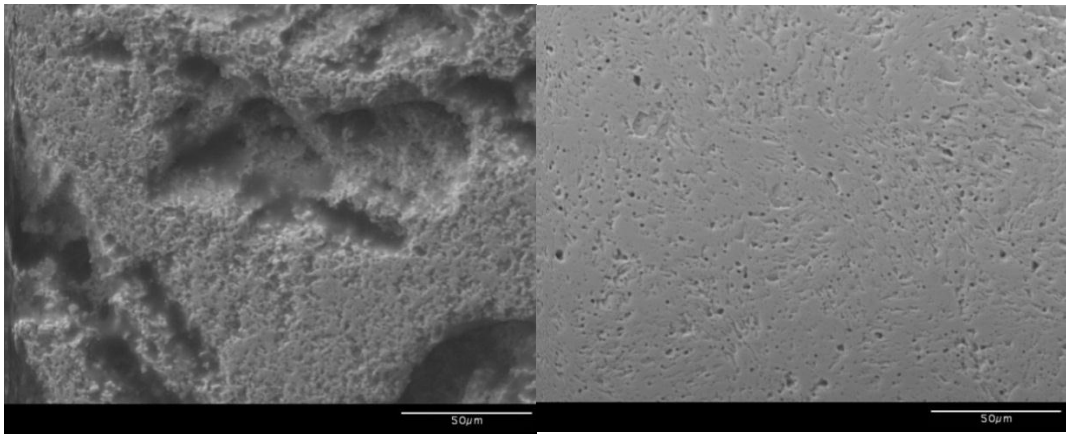

(i) **(j)**

Figure 3.7. SEM images of the micro-structure of (a). 50%ZrC+50%W, FEF fabricated; (b). 50%ZrC+50%W, isostatic pressed; c). 62.5%ZrC+37.5%W, FEF fabricated; (d). 62.5%ZrC+37.5%W, isostatic pressed; (e). 75%ZrC+25%W, FEF fabricated; (f). 75%ZrC+25%W, isostatic pressed; (i). 100%ZrC, FEF fabricated; (j). 100%ZrC, isostatic pressed (cont)

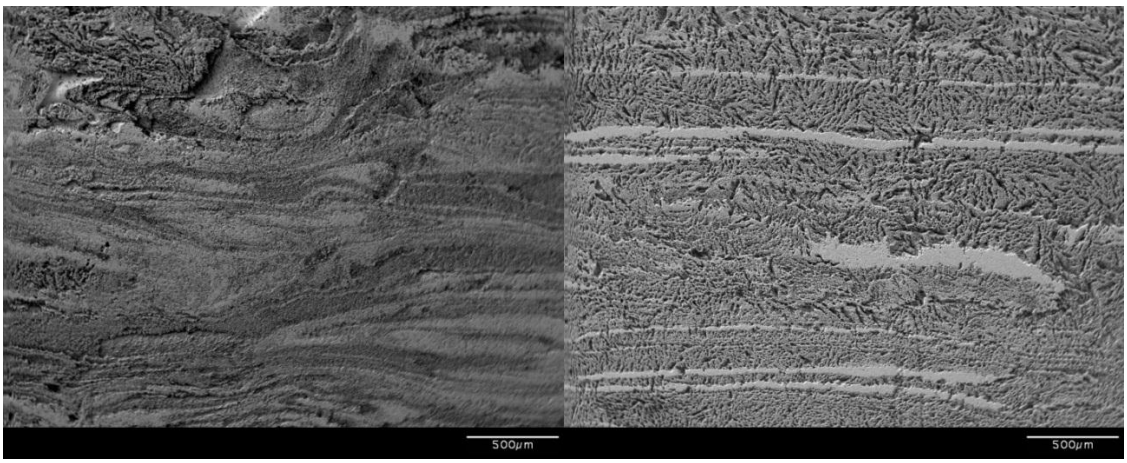

(a) **(b)**

Figure 3.8. SEM images of FEF test bars: (a). Cross section of 62.5%ZrC+37.5%W. (b). Cross section of 87.5%ZrC+12.5%W

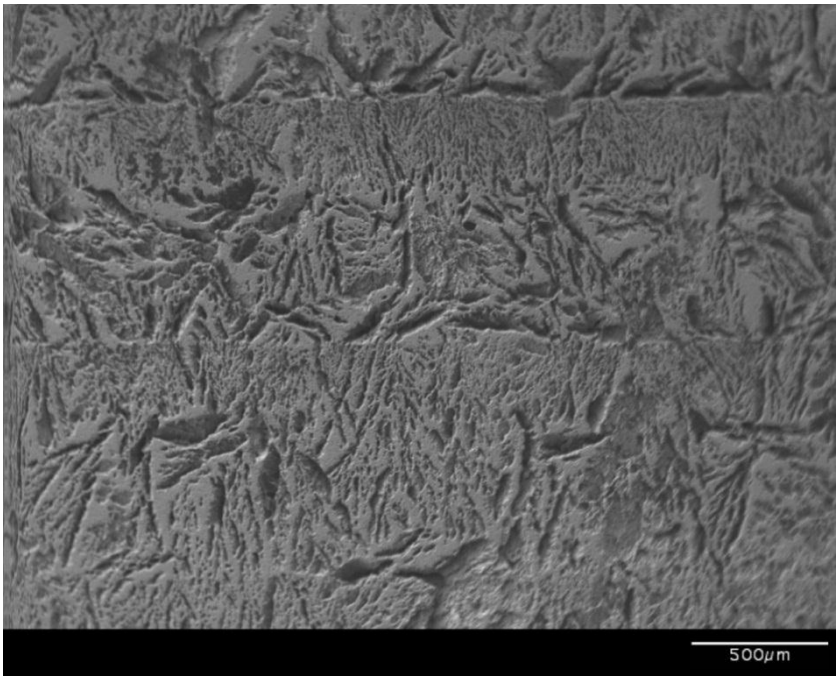

Figure 3.9. SEM image showing the formation of ice crystals in the FEF-fabricated 100%ZrC test bar

Glycerol could prevent the complete crystallization of ice by effectively binding to the water molecules, which leads to the formation of amorphous structure so that the growth of crystals could be inhibited [20]. To investigate the effect of glycerol on controlling the growth of ice crystal, two batches of alumina paste at the solids loading of 60 vol%, one with glycerol (the amount of glycerol is 20 wt.% of water) and one without glycerol (recipe provide in the appendix). Two samples were taken from each of the pastes and went through freeze-drying and then sintering. After polishing, the sintered samples were observed using scanning electron microscopy (SEM). Figure 3.10 (a) and (b) show the microstructures of samples with and without glycerol, respectively.

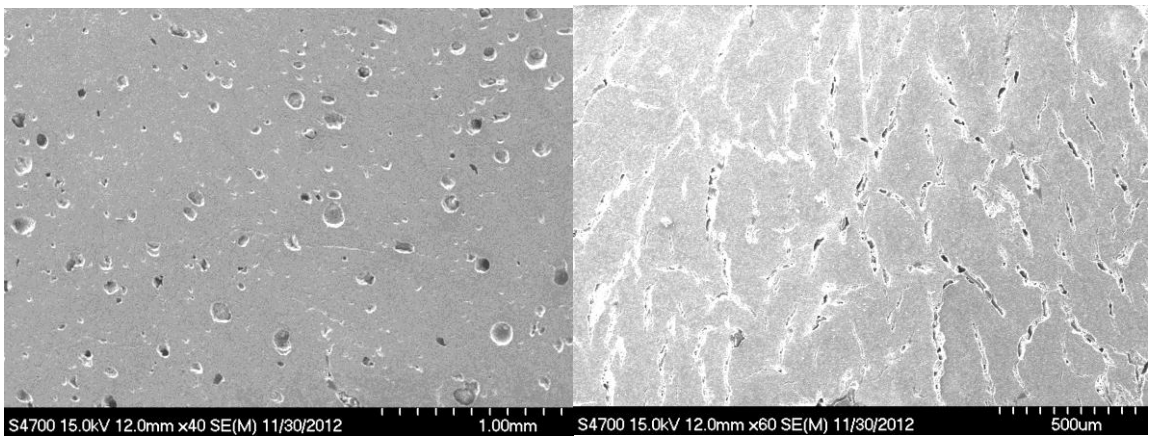

(a) **(b)**

Figure 3.10. (a) Microstructure of sample with use of glycerol in the paste; (b) Microstructure of sample without glycerol.

There is large difference in the microstructures of samples with and without glycerol. The glycerol added paste reveals the absence of freeze defects, while the other paste shows long cracks caused by the formation of icecrystals, which is believed to be more determined to the mechanical properties of sintered parts than the spherical voids in the glycerol added paste. In order to verify the hypothesis, a new batch of 50 vol.% ZrC paste with glycerol (20 wt.% of water) was made, then FEF test bars were extruded using the paste and went through all the post process. Figure 3.11 shows the comparison between the microstructure of FEF test bars made with and without glycerol. Under the same magnification, it is apparent that the size of the pores has been significantly decreased. Density and flexural strength were measured and listed in Table 3.8.

Table 3.8. Comparison of density and flexural strength between samples made with and without glycerol

With glycerol	Relative density	Flexural strength (MPa)
Yes	73.19%	82
No	62.05%	73

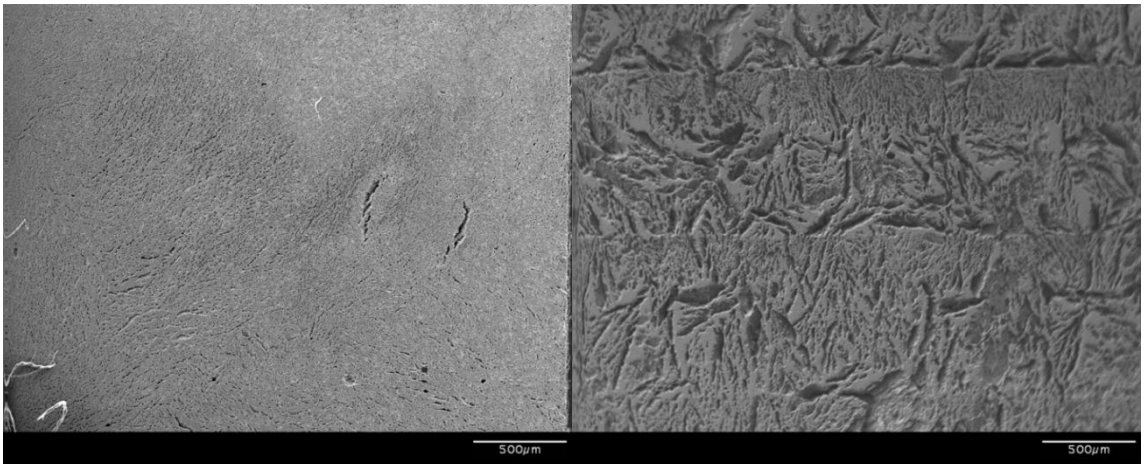

(a) **(b)**

Figure 3.11. (a) Microstructure of sample with glycerol in the paste; (b) Microstructure of sample without glycerol.

ImageJ software was used to measure the porosity in order to verify the density data and they corresponded well. The density and flexural strength data proved previous hypothesis that the addition of glycerol is helpful in controlling the ice crystals and enhancing mechanical strength by creating more nucleation sites during freezing, then reducing the size of ice crystals. And it has to be mentioned that due to mechanical problems, the FEF test bars made with glycerol actually had lots of large gaps in the body, which with no doubt would affect the density and flexural strength. With an ideal extrusion performance the performance of the FEF test bars would definitely be much better. Thus glycerol will be used in future paste process.

4. SUMMARY AND CONCLUSIONS

The pure aqueous based ZrC and 50 vol.% ZrC+50 vol.% W paste were successfully developed and implemented in the fabrication of functional gradient material. The difficulty of disperse W powder was solved by the use of sodium dodecyl sulfate (SDS) as the dispersant, and SDS was proved to be the optimum dispersant in the development of ZrC and W pastes. Also, glycerol showed its advantage in the paste development by avoiding the formation of ice crystal during the freeze drying process and decrease the viscosity of paste, which could be very helpful when making the pastes with W. And several paste recipes were made based on those research.

ZrC/W test bars having compositions ranging from 100% ZrC to 50%ZrC+50%W, by volume, were prepared by isostatic pressing and freeze-for extrusion fabrication (FEF). Using attrition milled ZrC powder, relative densities ranging from 94.4 to 99.8% could be achieved for isopressed and co-sintered ZrC and W compositions by sintering at 2300 ℃ a the heating rate of 10 ℃/min from room temperature to 2100 ℃, and then 2 ℃/min to 2300 ℃. However, FEF fabricated bars only achieved 47 to 70% relative density for similar compositions. Flexural strength in four-point bending followed a similar trend, with strengths in the range of 200 to 400 MPa for the dense isopressed bars and strengths of only 25 to 70 MPa for the bars produced by FEF processing. The large differences in both density and flexure strength between the isostatic pressed and FEF fabricated test bars were found to be due to large voids inside the FEF fabricated bars from the formation of ice crystals during the freezing process, and this problem was overcome by the introduction of glycerol in the paste. An improved mixing method is needed in order to enhance the performance of graded ZrC/W composites fabricated by FEF process .

REFERENCES

[1] J.P. Kruth, M.C. Leu, T. Nakagawa, Progress in Additive Manufacturing and Rapid Prototyping, CIRP Annals - Manufacturing Technology, 47(2) (1998) 525-540.

[2] G.N. Levy, R. Schindel, J.P.Kruth, , Rapid Manufacturing and Rapid Tooling with Layer Manufacturing (LM) Technologies, State of the Art and Future Perspectives, CIRP Annals - Manufacturing Technology, 52(2) (2003) 589-609.

[3] A. Bandyopadhyay, P. Panda, M. Agarwala, S. Danforth, A. Safari, Processing of Piezocomposites by Fused Deposition Technique, Journal of the American Ceramic Society, 80(6) (2000) 1366-1372.

[4] S. Crump, Apparatus and Method for Ceramic Three-Dimensional Objects, U.S. Patent, No. 5121329, 1992.

[5] G.E. Hilmas, J. Lombardi, R. Hoffman, Advances in the Fabrication of Functional Graded Materials Using Extrusion Freeform Fabrication, Solid Freeform Fabrication Symposium, University of Texas at Austin, August 1996.

[6] M. Cima, M. Oliveira, H. Wang, E. Sachs, R. Holman, Slurry-Based 3DP and Fine Ceramic Components, Proceedings of Solid Freeform Fabrication Symposium, 2001.

[7] J. Kruth, P. Mercelis, L. Froyen, M. Rombouts, Binding Mechanisms in Selective Laser Sintering and Selective Laser Melting, Proceeding of Solid Freeform Fabrication Symposium, 2004.

[8] M.C. Leu, E. Adamek, T. Huang, G.E. Hilmas, F. Dogan, Freeform Fabrication of Zirconium Diboride Parts Using Selective Laser Sintering, Proceedings of Solid Freeform Fabrication Symposium, 2008.

[9] J. Stampfl, A. Cooper, R. Leitgeb, Y. Cheng, F. Prinz, Shape Deposition Manufacturing of Microscopic Ceramic and Metallic Parts Using Silicon Molds, U.S. Patent, No. 6242163, 2001.

[10] J. Cesarano III, R. Segalmen, P. Calvert, Robocasting Provides Moldless Fabrication from Slurry Deposition, Ceramics Industry, 148 (1998) 94-102.

[11] G. He, D. Hirschfeld, J. Cesarano III, J. Stuecker, Processing of Silicon Nitride-Tungsten Prototypes, Ceramic Transactions, 114 (2000) 325-332.

[12] T. Huang, M.S. Mason, G.E. Hilmas, M.C. Leu, Freeze-form Extrusion Fabrication of Ceramic Parts, International Journal of Virtual and Physical Prototyping, 1 (2) (2006) 93-100.

[13] M.S. Mason, T. Huang, R.G. Landers, M.C. Leu, G.E. Hilmas, Aqueous-Based Extrusion of High Solids Loading Ceramic Pastes: Process Modeling and Control, Journal of Materials Processing Technology, 209 (6) (2009) 2946-2957.

[14] T. Huang, M.S. Mason, G.E. Hilmas, M.C. Leu, Aqueous Based Freeze-form Extrusion Fabrication of Alumina Components, Rapid Prototyping Journal, 15 (2) (2009) 88-95.

[15] X. Zhao, R.G. Landers, M.C. Leu, Adaptive Extrusion Force Control of Freeze-Form Extrusion Fabrication Processes, ASME Journal of Manufacturing Science and Engineering, 132 (6) (2010) 064504.

[16] N.D. Doiphode, T. Huang, M.C. Leu, M.N. Rahaman, D.E. Day, Freeze Extrusion Fabrication of 13-93 Bioactive Glass Scaffolds for Bone Repair, Journal of Material Science: Materials in Medicine, 22 (3) (2011) 515-523.

[17] S.W. Yih, C.T. Wang, 1979 Tungsten-Sources, Metallurgy, Properties and Application. Plenum Press, New York.

[18] G.M. Song, Y.J. Wang, Y. Zhou, The Mechanical and Thermophysical Properties of ZrC/W Composites at Elevated Temperature, Materials Science and Engineering: A, 334 (2002)223–232.

[19] S.C. Zhang, G.E. Hilmas, W.G. Fahrenholtz, Zirconium Carbide–Tungsten Cermets Prepared by In Situ Reaction Sintering, Journal of the American Ceramic Society, 90(6) (2007) 1930–1933.

[20] W.S. Stephen, F. Dogan, Freeze Casting of Aqueous Alumina Slurries with Glycerol, Journal of the American Ceramic Society, 84 (7) (2001) 1459–64.

[21] T. Oakes, P. Kulkarni, R.G. Landers, M.C. Leu,"Development of Extrusion-on-Demand for Freeze-form Extrusion Fabrication Processes," Proceedings of Solid Freeform Symposium, Austin, TX, 2009, pp. 206-218.

[22] S.W. Yih, C.T. Wang, Tungsten-Sources, Metallurgy, Properties and Application. Plenum Press, New York, 1979.

[23] X. Kou, S. Tan, "A Hierarchical Representation for Heterogeneous Object Modeling," Computer-Aided Design, 37 (2005), pp. 307-319.

[24] V.F. Petrenko, "Structure of Ordinary Ice Ih, Part I: Ideal Structure of Ice," Report No. 93–25, U.S. Army Corps of Engineers, Cold Regions Research and Engineering Laboratory, Hanover, NH, 1993.

APPENDIX

Recipes of ZrC and W paste at ~50% solids loading

1. Fill a 500 ml Nalgene bottle one-third of the way with ZrO_2 media.
2. Weigh out the powder(s) for the paste and pour them into the Nalgene bottle:
    a. ZrC paste – 465.5 g of ZrC
    b. ZrC/W paste – 673.75 g of W, 232.75 g of ZrC
3. Use a graduated cylinder to measure deionized water
    a. ZrC paste – 70ml
    b. ZrC/W paste – 120ml
4. Use a beaker and a scale to weigh out the correct amount of Sodium Dodecyl Sulfate (SDS) for the appropriate paste
    a. ZrC paste – 2.5 g of SDS+14g glycerol
    b. ZrC/W paste – 2.1 g of SDS
5. Pour the SDS into the Nalgene bottle. Use the water to rinse out the beaker into the Nalgene bottle.
6. Close the bottle and shake it by hand for a couple minutes until the contents turn into a slurry.
7. Ball mill for ~20 hours at ~35 rpm.
8. After ball milling, connect the water jacketed beaker to a water bath. Place the beaker at the bottom of a mechanical mixing machine. Set the water bath to 80 ℃. Do not remove the bottle off the ball mill until the water bath reaches 80 ℃.

9. Once the set temperature is reached, turn on the mixing machine and set it to lowest speed. Pour the slurry into the water jacketed beaker. Make sure the media does not fall into the beaker.
10. Cover the beaker with a piece of plastic.
11. While waiting for the water bath temperature to come back to 80 ℃, weigh out the correct amount of Methocel (Methocel*F4M, Dow Chemical Company).
    a. ZrC paste – 1.5 g of Methocel
    b. ZrC/W paste – 0.85 g of Methocel
12. Lifting the plastic cover with one hand, put a small amount of Methocel with a spatula in the other hand. Cover the beaker with the watch glass while the Methocel added is stirred into the slurry, the speed of mixer could be adjusted based on the mixing situation. Although the Methocel should be added slowly, the beaker should not remain uncovered for long since that will lead to water evaporation and the paste will not turn out as expected.
13. Once all the Methocel is added in, slow down the mixing speed to the lowest limit,
    a. ZrC paste – let the slurry stir for 5 minutes
    b. ZrC/W paste – open the cover and let the water evaporate for ~2 hours, take a small piece of sample every half an hour, put it in a small plastic plate and then dry it in a drying oven for half an hour to test the solids loading. Do not the evaporation until the solids loading reaches ~50%, then cover the beaker with plastic again

14. Set the water bath to 30 ℃. Make sure to check on it every once in a while. If a layer starts forming, stir the slurry with the spatula. The paste will start setting at ~40 ℃, then turn off the mechanical mixer.
15. When the water bath reaches 30 ℃, use the spatula to put the paste in the Whip Mixer container. Close it with the lid. Connect the vacuum line. Turn it on. Whip mix it for 5 minutes. Using a cooking spatula, scrape the paste off the blade. Whip mix it for another 3 minutes. Let it cool for 2 minutes. Whip mix it another 2 minutes for a total of 10 minutes.
16. Disconnect the vacuum line. Turn the Whip Mix on for a minute to clean the line and lubricate the motor.
17. Using a cooking spatula, put the paste in a bottle. Close it with a lid preferably. Otherwise, use parafilm.

    Make sure to take a small sample for solid loadings calculation

VITA

Ang Li was born in Changde, China in 1988. In 2006, he received his Bachelor of Science degree in Material Processing and Control from Huazhong University of Science and Technology, Wuhan, Hubei, China. In August 2010, he began his studies for the Master of Science degree in Manufacturing Engineering. In May, 2013, he received his Master's degree in Manufacturing Engineering from Missouri University of Science and Technology. His areas of interest include material science and ceramic/alloy processing.